RESEARCH ARTICLE

Structural Design, Optimization and Analysis of Robotic Arm Via Finite Elements.

Joseph Garikayi Kurebwa[1], Tawanda Mushiri[1]*

[1] Department of Mechanical Engineering, University of Zimbabwe, P.O Box MP167, Mt Pleasant, Harare, 00263, Zimbabwe.

Abstract: The study set out to determine the optimum architecture of a robotic arm link based on weight and payload and perform vibrational and stress analyses on the resultant shape. Findings showed the effectiveness of topology optimization in preliminary stages of structural design. The subsequent linear static analyses confirmed the degree of safety of the robotic arm links. It was also shown that that preload in the actuator wire incorporated in the links can be manipulated to tune the natural frequency of the structure. These findings contribute to the ongoing design of the entire robotic first aid system by providing data, which will be used for selection of components and inspire confidence to proceed with manufacture.

Keywords: Stress; robotic arm link; safety first aid; natural frequency; mode shape; passenger car; vibration; shape.

1. Introduction

When the sophisticated machines that man depends on for sustenance fail, they do so horrifically. Historically, human beings have shown nearly zero tolerance for injury or death caused by flaws inside a machine [1]. The advent of computer aided design (CAD) coupled with finite element analysis (FEA) as early as the mid-twentieth century has culminated in quick and increasingly accurate design and predictions of real world machine behaviour. In the past forty years, researchers have shown an increased interest in the finite element method (FEM) for stress analysis of machine components, both static and dynamic, prior to manufacturing [2]–[5]. Recent developments in the field have heightened the use of the FEA tools is used in vibrational and fatigue life analysis [6], [7]. Traditionally, products have been designed and analysed later in the development process, but in the past five years generative design via FEA has been getting much attention from modeling software developers, researchers and engineers. Not only does this alleviate waste from production of defective products, but it also quickens the product development process [8]. Finite element analysis is one of the most active areas in product research and development today.

In the context of the passenger car, which has several moving parts, it is necessary to ascertain the dynamic relationship of the Robotic First Aid (RFA) mechanics and the rest of the vehicle. For structural soundness of the robot and its reliability, this paper delves into key issues including stress and vibration. In addition to generative design of structural components, the paper specifically seeks to verify the degree of safety of the design as well as the operational natural frequencies of the robotic arm architecture. These data will serve as guidelines for further development of robotic arm components, whether mechanical or electronic, in the unchartered realm of robotic first aid systems for passenger car occupants.

doi: 10.18063/phci.v1i2.784

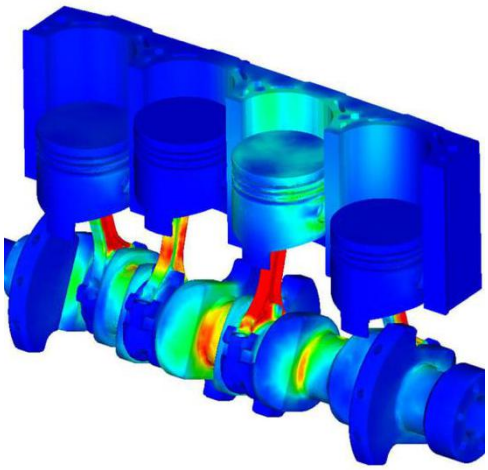

Figure 1. A depiction of finite element analysis of some components making up a four-stroke engine.

2. Literature Review

2.1 Structural Design Optimization

Design optimization is the process of establishing the right combination of product parameters that satisfy project requirements [9], [10]. In 2011, Zhou, Bai and Hansen published a paper in which they identified light-weightiness as the subject of their robot arm design optimization [11]. Femto Engineering in 2017 confirmed weight as a prime optimization parameter and added that structural design optimization could be categorized as sizing optimization, shape optimization and topology optimization [12]. The report highlighted that in sizing optimization, an optimum relation between weight, stiffness and the dynamic behaviour is found without changing the general shape of the geometry whereas shape optimization identifies the optimum shape of a structure by changing the surface geometry to minimize stress peaks to improve fatigue life. Topology optimization is a mathematical method that influences layout of material within a specific design space, for a specific set of loads, boundary conditions and constraints with the aim of maximizing performance of the system.

The integration of topology optimization methods into CAD has revolutionized the product development process by bringing stress analysis and factoring in manufacturing technology into the initial design phase. Autodesk has developed a shape generating tool integrated into its CAD software. The generative design tool mimics nature's evolutionary approach to design. Design goals are the inputs to the generative design software, along with parameters including materials and cost constraints, and optimized structures are the outputs. It appears from the literature that, considering the aim of this paper, topology optimization methods for weight reduction and increased stiffness can be applied to the RFA system's arm, with a predetermined payload as the design requirement.

Recently, Cunningham reported that there are two approaches to design optimization during FEA [13]. The first one is direct optimization, which uses the actual FEA results that are solved sequentially during optimization. The optimization algorithm determines the next design point's orientation from previous results and the iterations continue until a specified limit is reached. The other approach is that of response surface optimization. In this case, design point results generation precedes the optimization. The design point configurations are normally determined by design of experiments methods with the intention of using a minimum number of actual analysis runs to characterize the system response. When fit to the analysis data, the response surface functions serve as surrogate models, which the algorithm samples in search of the optimum design. The author writes that the latter approach is more advantageous than the former, particularly in simulation time and computational capacity. This resonates with findings by Rule in 1997, which showed that the response surface was more effective than conventional optimization algorithms [14]. The finding is consistent with findings of past studies by Yanhui, Ziyan and Zijian, who studied optimization of preform shapes by response surface and finite element methods to improve deformation homogeneity in aerospace forgings [15]. From

these studies, it can be concluded that the response surface optimization approach should be used in this research.

Various researches have validated and verified structural design optimization techniques for effective product development. In a study by Utpat *et al*., structural design optimization was based on the FEM and consisted of completion of the design model using dimensional data as design variables [16]. The important optimization considerations were minimum weight, maximum static stiffness and minimum deformation for maximum precision at the end effector. Topological optimization was carried out using Ansys topological optimization routine, resulting in reduced weight and deflection thus the robotic arm's performance was improved. In addition, Song, Kim and Jang checked the constraints of minimum weight design of racing motor boats and their results verified the applicability of structural optimization algorithms to actual structural design [17].

2.2 Modal Analysis

Modal Analysis is the processes by which the inherent dynamic characteristics of a particular system are determined and used to formulate a mathematical model representing the dynamic behavior of the system [18]. In the context of the robotic arm in question, it can also be defined as the study of the dynamic properties of the arm in the frequency domain. In the past four decades it has become a major technological tool in the quest for determination, improvement and optimization of dynamic characteristics of engineering structures [18]. Accordingly, modal analysis is an indispensable step in the RFA system's design considering vibration-inducing loads from vehicle movement.

Researchers have used modal analysis to determine the safe operational frequencies in various systems. In 2016, He and Guo demonstrated the use of modal analysis of a humanoid robot arm in identifying corresponding modal frequencies and more importantly, pointing out the potential dangerous operating conditions of the robot arm [19]. Success of modal analysis method was reiterated by Sahu, Choudhury and Biswal, who analysed various modes of frequencies of a robot and determined its weak parts using the FEM [20].

The present study presents an interesting scenario where the structural components are bound together by pre-tensioned connectors. There is a considerable amount of research on the setup, with agreement that there is a relationship between preload and natural frequency. It has been shown by Lu, Xu and Liu that single order frequencies decrease with an increase in preload force, and that preload forces have a greater effect on low-order frequencies than high order frequencies [21]. The use of the FEM in modal analysis by the authors also endorses the methodology in the present study, resonating with Xu and Hess's experimental results, which show a 1-2% decrease in natural frequency at low levels of preload [22]. It is therefore well-founded that the present study investigates the effect of preload on the robotic arm link's natural frequency with the expectation of the aforementioned relationship.

3. Materials and Methods

3.1 Loading

Only the configurations with the highest anticipated load on robotic arm link components were considered in the design and analyses. The robotic arm conceptual design comprised six links. The first load case was one where a robotic arm link was required to lift the end effector combined with the links preceding it. Such an arrangement is analogous to a cantilever. The torque required at the pivot was calculated using the principle of moments.

For 184mm long links weighing 300g each, coupled to an end effector with the same physical properties, the torque required to lift the robotic arm links is presented in Table 1. It should be noted that central location of each link's center of gravity was assumed. Moreover, the heaviest of all 6 linkages weighed 250g, and another 50g were included in anticipation of weight of additional components for functionality of the robot, such as sensors and cables.

In the second load case, the robotic arm link immediately preceding the one in question was assumed to be articulated at 90°, and all others before it unarticulated. The configuration resulted in induction of torsion in the present link. A little consideration will show that the twist torque at each joint was equal to lift torque in Table 1. It should be noted that the maximum articulation angle of any link in any direction was 45° in an embodiment of the present

disclosure, making the values in the table slightly greater than the actual.

Member	Lift / Twist Torque (Nm)
Link 1	0.271
Link 2	1.083
Link 3	2.436
Link 4	4.332
Link 5	6.769
Link 6	9.747

Table 1. Lift and twist torque acting on the linkages.

Referring to Table 2 and **Figure 2**, the member was fix-constrained at the green surfaces, thus there were zero degrees of freedom. Load P was applied at the blue and yellow surfaces in the positive and negative X-axis respectively. W represent the weight of all members preceding its point of application, which was the yellow surfaces in the negative Y direction. The torsion torque was depicted by the couple of forces M_1 and M_2, applied in opposite directions along the Y-axis on the yellow surfaces and acting 22mm from the axis of the cylindrical links. It should be noted that there were no M_1 and M_2 loads on links 5 and 6 because in an embodiment of the present disclosure, the members were not exposed to the torsion load.

Member	P (N)	W (N)	M1 = −M2 (N)	Preload (N)
Link 1	27.1	2.94	6.16	5.02
Link 2	108	5.89	24.6	10.0
Link 3	244	8.83	55.4	14.0
Link 4	433	11.8	98.5	20.1
Link 5	677	14.7	-	25.1
Link 6	975	17.7	-	27.9

Table 2. Loads acting on the robotic arm links.

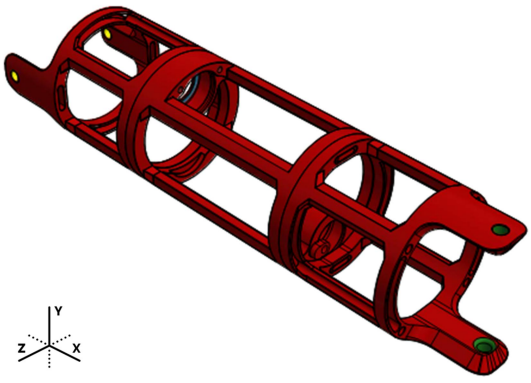

Figure 2. Points of application of loads acting on the robotic arm links.

3.2 Generative Design

Generative design of the structural segments was carried out in Autodesk Inventor's Shape Generator. Firstly, an approximation of the part model was created as shown in **Figure 2.** Since the tool analyses parts and not assemblies, the three members were first merged in the Inventor part environment. Preserve or keep-out zones were then defined, and the forces and constraints on the part were applied. The Shape Generator study was run, resulting in removal of excess material and presentation of the refined part's generalized shape. It should be noted that the tool was run twice, first for

the bending load then for torsion. Finally, the part was modified accordingly.

3.3 Linear Static Analysis

To verify the shape generator's solution, the link assembly was analysed for stress under the loads in Table 2, with the following assumptions:

displacements and rotations were small,

supports did not settle

material remained linear, and stress was directly proportional to strain, and

loads (magnitude, orientation, distribution) remained constant as the structure deformed.

Therefore, the study was linear. The simulation workflow was as follows:

The assembled first robotic arm link was opened in Autodesk Inventor, and the Nastran In-CAD environment was loaded.

Idealizations for the yoke and mount segments were defined as Aluminium 6061.

Separation surface contacts were added to the assembly's contact surfaces.

Constraints and loads were applied to simulate the real world. It should be noted that loads P, and M_1 and M_2 were mutually exclusive as they represented two loading extremes by the same components. Furthermore, cable connectors could have been added to represent the preloaded shape memory alloy (SMA) actuator wire, but they would have been included in the results for factor of safety. This would have result in ambiguous results given that the wire's material was user-defined and unconfirmed to be accurate.

Finally, the model was meshed, and the simulation was run.

The studies were run for the second to sixth links, with the preloads increasing from 69.8 N to 175 N in multiples of 34.9 N. A little consideration will show that as the number of links increased, the tension in the wires binding the yoke and mount segments also needed to increase (from the end effector to the base), thus multiplication of the preload.

3.3 Modal Analysis

Since mode shapes will change given that the masses used for simulation were only approximations, the deviation of the actual natural frequency from the actual was assumed to be marginal. Normal modes and Prestress normal modal analyses in Autodesk Nastran In-CAD were carried out on the linkages to verify the relationship between bolt preload and natural frequency of structural members. The workflow of the modal analyses was akin to that of the linear static analyses, with the addition of the following considerations:

The analysis type was changed from the default "Linear Static" to either "Normal Modes" or "Prestress Normal Modes". Notably, these analyses are both linear and the assumptions made in the linear static study were valid.

Bolt connectors were used, with no preload in the normal modes analyses and with preload in the prestress normal modes analyses.

External loads were not applied since they did not affect natural frequency of the links.

4. Results

4.1 Topological Optimisation

The masses of the three segments under investigation were significantly reduced. **Figure 3** below shows the evolution of the components from their initial to their final geometries, whose physical properties are presented.

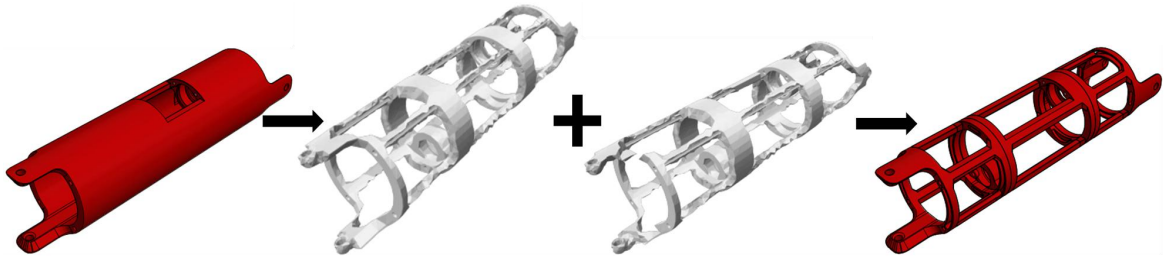

(a) *(b)* *(c)* *(d)*

Figure 3. Evolution of the robotic arm link's architecture from the initial concept (a) through generative design for bending (b) and torsion (c) to the optimized shape (d).

4.2 Prestress Static Analysis

The results from the linear static analyses indicate design compliance for all components across the six links, with factors of safety well above 1. The studies also revealed marginal deformation displacements in the members under load as shown below. Table 3 shows the maximum displacements and Von Mises stresses, as well as minimum safety factors for the members, due to the lifting load. Similarly,

Table 4 shows the same indicators, but for the torsion load.

Member	Maximum Solid von Mises Stress (MPa)	Maximum Displacement (mm)	Minimum Factor of Safety
Link 1	11.8	0.024	24.14
Link 2	30.2	0.0585	12.3
Link 3	35.6	0.0486	10.8
Link 4	123	0.202	3.01
Link 5	115	0.292	3.17
Link 6	163	0.397	2.27

Table 3. Maximum von Mises stress, maximum displacements and minimum safety factor results for bending load.

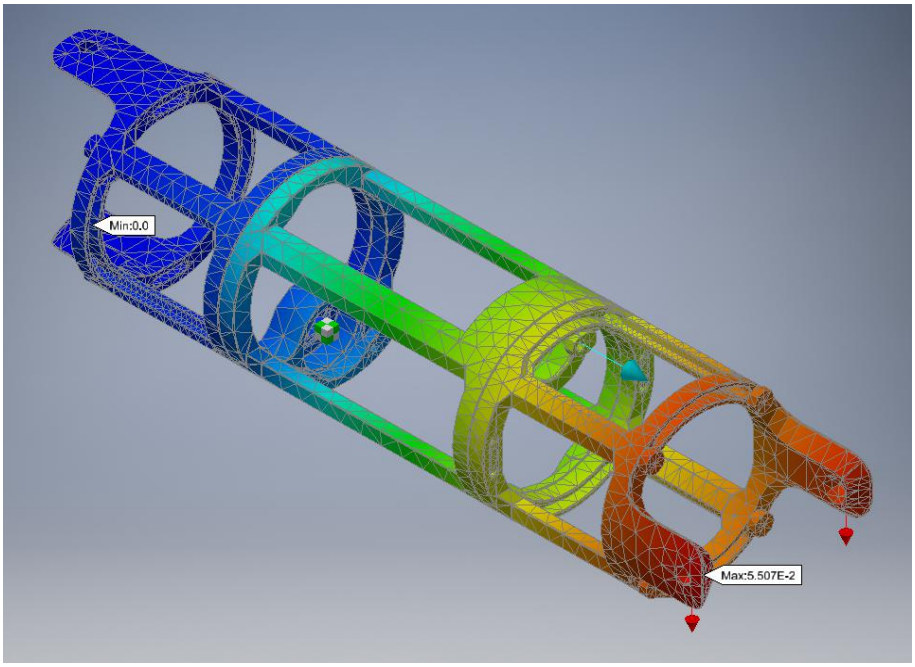

Figure 4. Mode of bending deformation depicted by displacement, where the shade approaches red with increase in displacement.

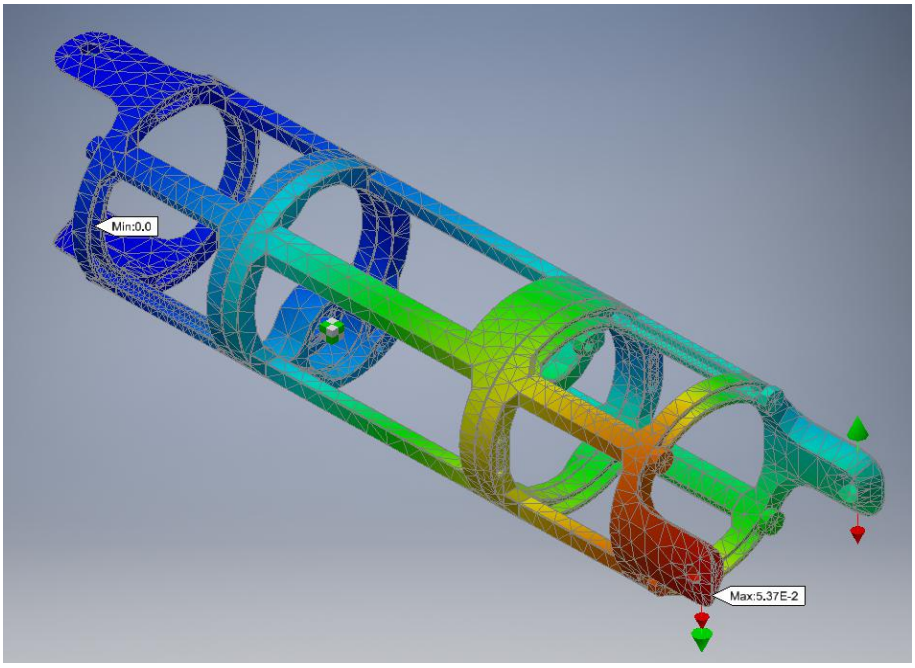

Figure 5. Mode of torsional deformation depicted by displacement, where the shade approaches red with increase in displacement.

Member	Maximum von Mises Stress (MPa)	Maximum Displacement (mm)	Minimum Factor of Safety
Link 1	10.2	0.037	40.5
Link 2	37.4	0.118	11.1
Link 3	56.4	0.198	7.45
Link 4	94.1	0.326	4.3

Table 4. Maximum von Mises stress, maximum displacements and minimum safety factor results for torsion load.

4.3 Modal Analysis

As expected, the different links with different masses and shapes also have various normal mode shapes. Likewise, links with similar geometry such as links 1 to 4 also have comparable normal mode natural frequencies. Furthermore, there is a notable difference between preloaded and non-preloaded link natural frequencies. The first ten mode shapes for the various values of preload in the SMA actuator wire are summarized in Table 5 and illustrated in **Figure 6.**

Mode	Frequency (Hz)							
Analysis	Normal Modes		Prestress Normal Modes					
Member	Links 1 – 4	Links 4 & 5	Link 1	Link 2	Link 3	Link 4	Link 5	Link 6
Preload (N)	0	0	5.02	10.0	14.0	20.1	25.1	27.9
1	300.95	290.26	304.56	304.25	303.85	302.97	293.95	293.94
2	571.87	564.92	575.56	580.05	581.12	581.77	566.95	566.96
3	1200.13	1145.15	1207.22	1206.76	1205.62	1202.91	1147.55	1147.55
4	1693.23	1764.11	1696.50	1730.83	1736.03	1741.48	1766.14	1766.13
5	2037.22	2095.81	2037.68	2076.52	2080.11	2083.17	2092.29	2093.60
6	2425.43	2492.31	2427.63	2461.13	2465.94	2470.61	2478.44	2479.70
7	2575.86	2619.97	2575.17	2609.07	2611.98	2614.86	2613.46	2616.64
8	2631.24	2643.71	2636.07	2643.19	2640.74	2635.71	2627.18	2627.61
9	3193.13	3201.14	3194.86	3189.16	3180.60	3164.82	3178.65	3178.55
10	3258.30	3253.74	3259.11	3269.84	3263.35	3257.54	3241.44	3241.79

Table 5. First ten modes and corresponding natural frequencies for preloaded and non-preloaded robotic arm links.

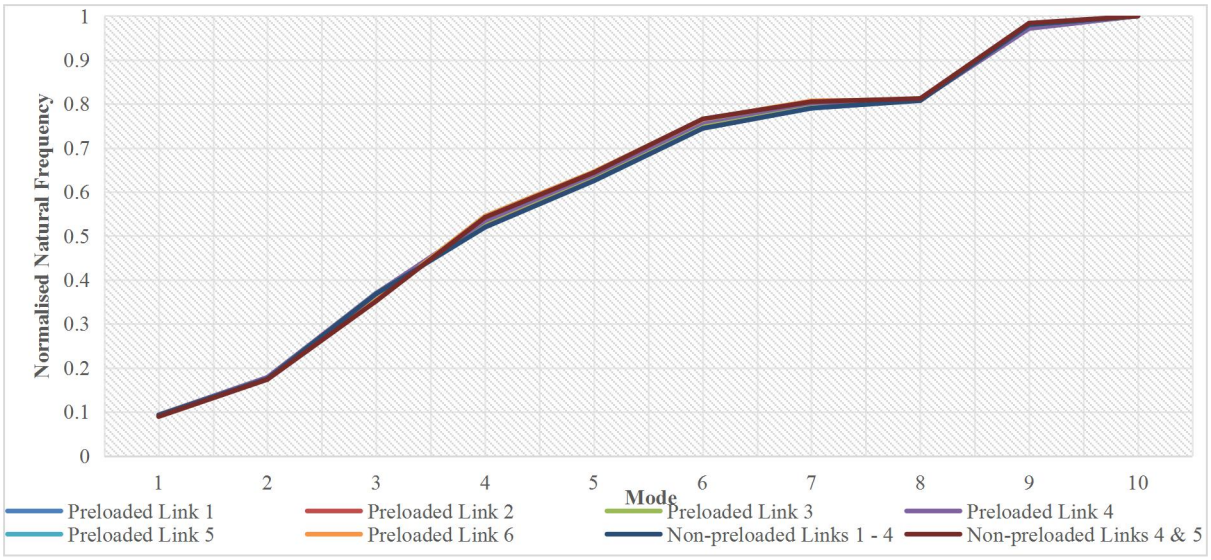

Figure 6. Normalised natural frequencies for preloaded and non-preloaded robotic arm links.

5. Discussion, recommendation and conclusion

The discussion of the results begins with structural design optimization. The significant reduction in weight while maintaining the payload confirmed the effectiveness of the shape-generating tool by Autodesk. However, the software could handle parts only and not assemblies and consequently the parts had to be merged prior to analysis. This implies that contacts between the mating surfaces were disregarded in shape generation. Furthermore, the software did not consider the manufacturing process, which was additive manufacturing in an embodiment of the present disclosure. This would have shown the areas in need for supports in 3D printing as an indicator of the actual manufacturing cost. Notwithstanding the slight discordance in shape generation, stress analysis confirmed the structural soundness of the generated shape and the final product appeared to be well sustained.

The linear study findings indicated design compliance of the robotic arm links. Vast differences in the safety factors for the various links were also observed as expected, and they present an opportunity for further individual link optimization instead of the one-size-fits-all approach employed in this paper. The small displacements also justify the assumptions made in carrying out the studies. Another important finding was the mode in which the structure deformed to give these displacements. These modes are vital for control systems, which can be designed to compensate the deformation.

The modal analysis results showed a consistent relationship between the SMA actuator wire preload and the natural frequency of the robotic arm link. It can be seen in Table and Figure that the frequency decreases with increase in preload, which confirms previous studies [21]–[23]. This finding presents the possibility of manipulating the natural frequency of the robotic arm by altering preload. Since vehicle frequency is continuously varying, the natural frequency of the robotic arm can be controlled to avoid resonance, which could result in excessive vibrations thereby damaging the robot's components.

Unlike the advanced Nastran In-CAD topological optimization tool add-in, the shape generator does take the part's manufacturing process into consideration. Further work needs to be carried out encompassing additive manufacturing (3D printing), which is considered the appropriate manufacturing technology.

6. Conflict of interest

No conflict of interest was reported by all authors.

References

1. Toyota USA, Toyota CES 2017 Live Stream. Toyota USA, 2017.
2. N. S. Rothman and J. A. Ecker. Computer-Aided Engineering for Structural Analysis. Johns Hopkins APL Tech.

Dig., 1986; 7(3): 256–259.
3. K. K. Gupta and J. L. Meek. A Brief History of the Beginning of the Finite Element Method. Int. J. Numer. METHODS I N Eng., 1996; 39: 3761–3774.
4. I. Holand. Application of Finite Element Methods to Stress Analysis. in Numerical Solution of Partial Differential Equations, 1973: 195–221.
5. R. W. Clough. Early history of the finite element method from the view point of a pioneer. Int. J. Numer. Methods Eng., 2004; 60(1): 283–287.
6. G. Wu, W. Shi, Z. Chen, J. Fu, N. Guo, and S. Hou. Finite element modal analysis and test modal analysis of the control cab. in Proceedings of 2011 International Conference on Electronic & Mechanical Engineering and Information Technology, 2011: 2109–2111.
7. P. Schwibinger and R. Nordmann. Torsional Systems: Vibration Response by Means of Modal Analysis. in Rotordynamics 2, 2nd ed., Rieger N.F., Ed. Vienna: Springer, 1988: 331–357.
8. M. Tisza and Z. Lukács. Rapid Parametric Process Design Using FEM Analysis. Adv. Mater. Res., 2005; 6(8): 235–240.
9. MathWorks. Design Optimization with MATLAB and Simulink. MathWorks, 2018. [Online]. Available: https://www.mathworks.com/discovery/design-optimization.html. [Accessed: 19-Apr-2018].
10. R. Roy, S. Hinduja, and R. Teti. Recent advances in engineering design optimisation: Challenges and future trends. CIRP Ann., 2008; 57(2): 697–715.
11. L. Zhou, S. Bai, and M. R. Hansen. Design optimization on the drive train of a light-weight robotic arm. Mechatronics, 2011; 21(3): 560–569.
12. Femto Engineering. Structural Design Optimization Techniques & Tools - Femto Engineering. Femto Engineering, 2017. [Online]. Available: https://www.femto.eu/stories/design-optimization/. [Accessed: 19-Apr-2018].
13. P. Cunningham. Two Approaches to Design Optimization During Finite Element Analysis. Engineering Advantage Blog, 2014. [Online]. Available: https://caeai.com/blog/design-optimization-finite-element-analysis. [Accessed: 19-Apr-2018].
14. W. K. Rule. A Response Surface for Structural Optimization. J. Offshore Mech. Arct. Eng., 1997; 119(3): 196.
15. Y. Yanhui, L. Dong, H. Ziyan, and L. Zijian. Optimization of Preform Shapes by RSM and FEM to Improve Deformation Homogeneity in Aerospace Forgings. Chinese J. Aeronaut., 2010; 23(2): 260–267.
16. L. S. Utpat, D. K. Chavan, N. Yeolekar, A. Sahasrabudhe, and S. Mandke. Design Optimization of Robotic Arms. Int. J. Eng. Res. Technol., 2012; 1(3): 1–9.
17. H. C. Song, T.-J. Kim, and C. D. Jang. Structural design optimization of racing motor boat based on nonlinear finite element analysis. Int. J. Nav. Archit. Ocean Eng., 2010; 2(4): 217–222.
18. J. He and Z.-F. Fu, Modal analysis. Butterworth-Heinemann, 2001.
19. D. He and Y. Guo. Finite element analysis of humanoid robot arm. in 2016 13th International Conference on Ubiquitous Robots and Ambient Intelligence (URAI), 2016: 772–776.
20. S. Sahu, B. B. Choudhury, and B. B. Biswal. A Vibration Analysis of a 6 Axis Industrial Robot Using FEA. Mater. Today Proc., 2017; 4(2): 2403–2410.
21. A. Lu, J. Xu, and H. Liu. Effect of a preload force on anchor system frequency. Int. J. Min. Sci. Technol., 2013; 23(1): 135–138.
22. W. Xu and D. P. Hess. Effect of Fastener Preload on Structural Damping. J. Fail. Anal. Prev., 2013; 13(6): 744–747.
23. M. A. Chowdhury, M. Ali, and M. M. Helali. The effect of natural frequency of the experimental set‐up on the friction coefficient. Ind. Lubr. Tribol., 2010; 62(2): 78–82.